Proceedings of the ASME 2018
International Mechanical Engineering Congress and Exposition
IMECE2018
November 9-15, 2018, Pittsburgh, PA, USA

IMECE2018-88377

HEAT TRANSFER BY A ROTATING LIQUID JET IMPINGEMENT COOLING SYSTEM

Qi Lu, Siva Parameswaran, Beibei Ren
Department of Mechanical Engineering
Texas Tech University
Lubbock, Texas, United States

ABSTRACT

The circular, liquid jet impingement provides a convenient way of cooling surfaces. To effectively cool the devices inside the electric vehicle, a rotating jet impingement cooling system is designed to evaluate the potential of the jet impingement for high heat flux removal. The liquid used for jet impingement is automatic transmission fluid. The jet impingement system consists of a rotating pipe with two nozzles and a cylindrical ring which is attached to the heat source. To reduce the computational loads, first, the CFD simulation for a laminar flow inside the pipe is carried out to estimate the flow velocities at the nozzle exits. Then, the rotating jet impingement cooling of a cylinder with a uniform surface temperature is investigated numerically for stable, unsubmerged, uniform velocity, single phase laminar jets. The numerical simulation using the commercial code is performed to determine the heat flux removal performance over the cylindrical surface. The numerical results are compared with the empirical formula and experimental measurements from the literature. Furthermore, the effects of the Reynolds number and pipe rotation on the jet impingement cooling performance are also investigated.

INTRODUCTION

In recent years, with the development of the power electronics and battery technology, the electric vehicle (EV) has been widely applied in daily life. Compared to a traditional vehicle which is driven by an internal combustion engine, the advantages of the EV includes lower running costs, lower maintenance costs and less pollution to the environment. However, with the running of the EV, the electric motors and associated power electronics generate high-density thermal energy. These devices require efficient heat removal techniques to preserve their integrity and ensure their safe and reliable operation [1]. The high heat load in EV motivates the development of various cooling techniques, such as micro-channel cooling [2], spray cooling [3, 4] and jet impingement cooling [5, 6].

The liquid jet impingement cooling has gained lots of popularities due to the fact that it offers the high heat flux removal capability with a relatively simple implementation [7]. With a straight tube or contracting nozzles, a liquid jet impingement system could be easily created. Usually, no modification is needed on the target surface. When the jet hits the target surface, a stagnation zone is created, where a liquid film is formed which offers high heat removal performance [8]. Generally, impinging jets can be categorized as free-surface or submerged jets based on the species of the ambient fluid [9]. The heat transfer coefficient is also a complex function of various parameters, such as the Reynolds number, the Prandtl number of the fluid, the dimensionless jet-to-target spacing, the physical geometry of target and the relative motion of target [6]. In [10], experiments are performed to study the heat transfer of a round jet impinging on a flat plate with a constant heat flux rate. Effects of the jet Reynolds number, the nozzle to plate spacing and the jet diameter on heat transfer are investigated. Increasing the nozzle spacing generally decreases the Nusselt number. Correlations for the local and average Nusselt numbers revealed a Nusselt number dependence on the Reynolds number. A detailed review about the free surface, circular liquid jet is provided in [7]. Both theoretical and experimental results are developed. The target geometry will impact the flow topology when jet strikes the target surface. The heat transfer performance with the curved target surface is investigated numerically and experimentally in [11, 12, 13]. It is shown that the curved target surface could increase the heat transfer rate compared to the flat target surface. However, the working fluid in [11, 12, 13] for jet impingement cooling is air while in this paper the performance of the liquid jet impingement is investigated. The impact of target motion on the heat transfer of the jet impingement is investigated in [14]. The heat transfer is enhanced with the target rotation by generating a secondary flow.

In this paper, the heat transfer performance for a novel rotating liquid jet impingement cooling system is studied using numerical simulation. The jet impingement system consists of a rotational pipe with two nozzles. The target is a cylindrical ring, which contains curved target surfaces. Empirical formula [7] and experimental results [13] from the literature is used to validate

the numerical results. The effect of pipe rotation on the heat transfer performance is also revealed.

Compared to the existing literature regarding the jet impingement cooling system, the novelties of this paper lie in two aspects. Firstly, in the literature, the working fluid for the jet impingement cooling with the concave target surface is usually air. While in this study, the liquid jet impingement performance on the concave target surface with the working fluid of automatic transmission fluid (ATF) is investigated. Secondly, the effect of the pipe rotation on overall heat transfer performance is studied. Compared to the existing literature, where the target surface is rotating, this paper considers rotating the nozzles.

NOMENCLATURE

C_p	specific heat of the ATF (J/kg•K)
d	nozzle exit diameter (m)
D_1	outer diameter of the pipe (m)
D_2	inner diameter of the ring (m)
k	thermal conductivity of the ATF (W/m•K)
Nu_d	local Nusselt number based on jet diameter
$\overline{\mathrm{Nu}_d}$	average Nusselt number
$\widehat{\mathrm{Nu}}_d$	normalized local Nusselt number
$\mathrm{Nu}_d^{\max}$	maximum local Nusselt number
$\mathrm{Nu}_d^{\min}$	minimum local Nusselt number
Pr	Prandtl number of the ATF
q_w	wall heat flux (W/m^2)
Q_{inlet}	volume flow rate at the ATF inlet (m^3/s)
Re_d	jet nozzle Reynolds number
r	nozzle exit radius (m)
s	arc length from the center of the stagnation point along the wall (m)
T_w	wall temperature (K)
T_f	temperate of the liquid at the jet nozzle (K)
v	uniform axial velocity at the jet nozzle (m/s)
w	width of the fluid domain (m)
x	x coordinates of the fluid domain geometry, where the origin is at the geometric center (m)
ρ	density of the ATF (kg/m^3)
μ	dynamic viscosity of the ATF (Pa•s)
Ω	rotation speed of the rotational pipe (rpm)
σ_{Nu_d}	standard deviation of the Nusselt number

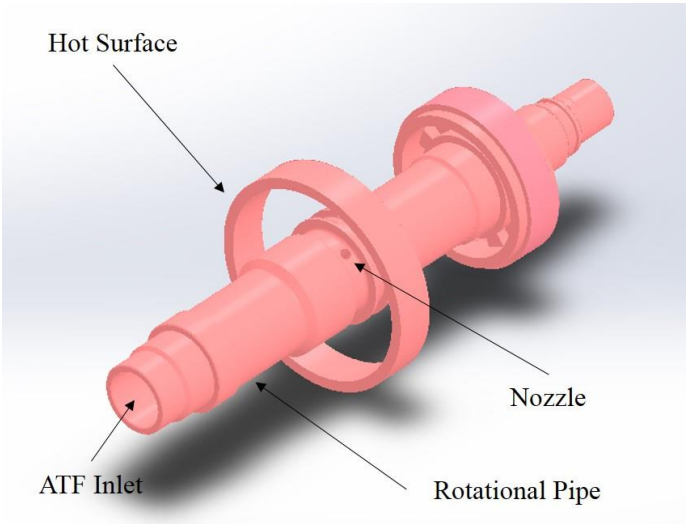

Figure 1 Schematic representation of the rotating liquid jet impingement cooling system

ANLYSIS MODEL AND METHOD

Analysis Model

The 3D model of the jet impingement cooling system is shown in Fig. 1. The hot cylinder is cooled using ATF by single-phase jet impingement cooling. Since the focus of this paper is about the heat transfer performance of jet impingement cooling system, in order to reduce the computational load, the laminar flow characteristics inside the pipe and the jet impingement cooling of the cylindrical ring are studied separately. First, the pressure drop between the ATF inlet and the nozzles is estimated by assuming that the pipe is static. Then the exit velocities at the nozzles are calculated from conservation of mass and Bernoulli's equation. The volume flow rate at the ATF inlet is $Q_{\mathrm{inlet}} = 8$ LPM and the jet exit flow velocities are $v = 3.3$ m/s. The model of the fluid domain used for simulating the jet impingement process along its main parameters are shown in Fig. 2, where s is the arc length along the cylindrical wall, $w = 0.018$ m is the width of the fluid domain, $d = 0.005$m is the nozzle exit diameter, $D_1 = 0.038$ m and $D_2 = 0.08795$ m are the outer diameter of pipe and the inner diameter of ring, respectively. The definition of the coordinates is shown in the lower left corner of Fig. 2.

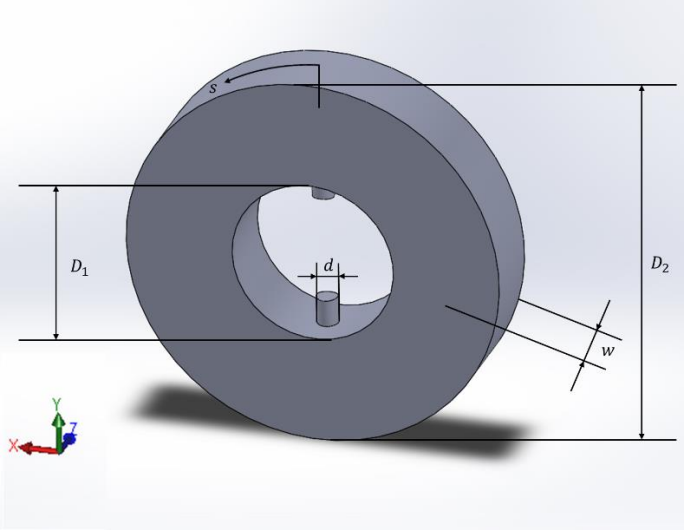

Figure 2 3D model of the fluid domain used for simulating the jet impingement process

Mesh and Boundary Condition

The details of the mesh are shown in Fig. 3. The commercial code is adopted to simulate the heat transfer and flow field for the jet impingement process. The operating pressure is set to one atmosphere pressure. The ATF at $T_f = 313.15$ K is impinging from the nozzles. At the inlet, the velocity-inlet boundary is

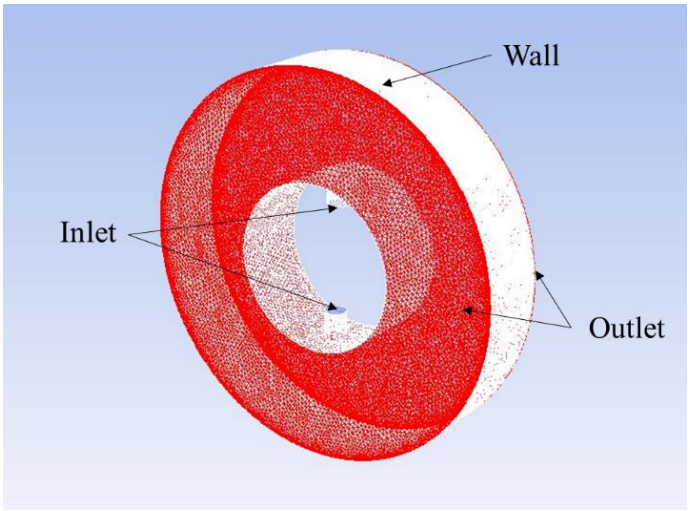

Figure 3 Computational mesh

adopted with the uniform axial speed set to $v = 3.3$ m/s and the pressure-outlet condition is used with the relative pressure set as zero. On the cylindrical wall, constant temperature is adopted with the setting of $T_w = 453.15$ K as the heated target surface. The RNG $k-\varepsilon$ model along with the two-layer near-wall treatment is employed as the turbulence model for numerical simulation [11]. Since the jet impingement process involves the interaction between the working fluid and air. The volume of fluid (VOF) method is adopted for multiphase modelling and the energy equation is used to solve the heat transfer process.

Grid Sensitivity Analysis

The steady-state numerical simulation studies with the static mesh are performed to conduct the grid sensitivity analysis, where the governing equations are solved in a stationary framework. The jet impingement flow field and the heat transfer performance are simulated with five different mesh schemes. The mesh refinement is applied especially at the wall, where the high heat flux gradients are expected. Since this paper mainly discusses the heat transfer performance, the results of the grid sensitivity analysis are demonstrated through the wall heat flux. The number of elements and the maximum wall heat flux for each mesh scheme are shown in Table 1.

TABLE 1 MESH SCHEMES AND WALL HEAT FLUXES

Scheme	Number of elements	Maximum wall heat flux (W/m^2)
Mesh 1	267,387	281,121
Mesh 2	851,277	497,899
Mesh 3	1,458,626	612,649
Mesh 4	1,946,167	631,385
Mesh 5	2,428,170	599,881

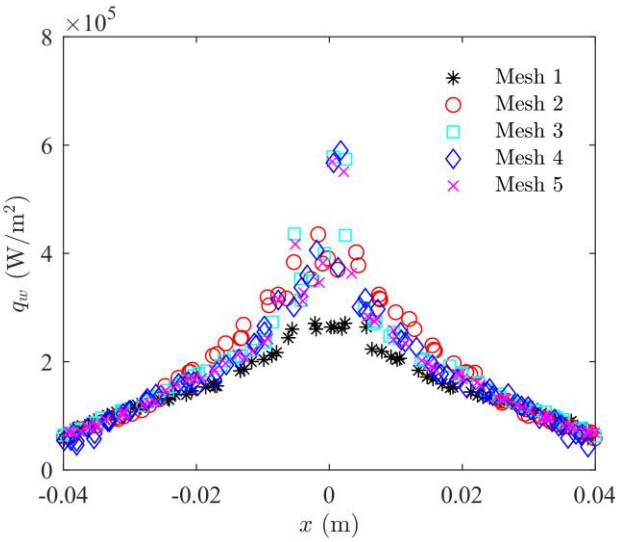

Figure 4 Grid sensitivity analysis-wall heat flux

Figure 4 shows the wall heat flux distribution at different x coordinates for five mesh schemes. 100 samples of the wall heat flux are taken for each mesh scheme. From Fig. 4 and Table 1, it could be seen that the Mesh scheme 4 possess the highest maximum wall heat flux. Furthermore, increasing the grid number does not contribute to finer heat transfer performance. Thus, the Mesh scheme 4 is used to conduct the numerical simulation to obtain the grid-independent results.

RESULTS AND DISCUSSION

Validation of Numerical Codes with Empirical Formula

Usually, the stagnation zone carries the highest Nusselt number. In order to validate the numerical results, the stagnation zone Nusselt number from the CFD simulation and the prediction of the empirical formula for uniform velocity profile laminar jets from [7] are compared. The empirical formula for stagnation point Nusselt number is

$$\mathrm{Nu}_d = 0.745\mathrm{Re}_d^{\frac{1}{2}}\,\mathrm{Pr}^{\frac{1}{3}} \tag{1}$$

where Nu_d is the Nusselt number, Re_d is the Reynolds number of the circular jet and Pr is the Prandtl number of the liquid. The above formula is derived based on theory and experiments with cold water and it applies to liquids with Prandtl numbers above 3. In the numerical simulation, the properties of the ATF are set as constant, which are evaluated as the average of the wall temperature and the liquid temperature at the nozzle exit. The properties of the ATF used in the numerical simulation are shown in Table 2.

TABLE 2 PHYSICAL PROPERTIES OF THE ATF

Physical properties	Value
Density, ρ	792 kg/m^3
Specific heat, C_p	2237 J/kg•K
Thermal conductivity, k	0.135 W/m•K
Dynamic viscosity, μ	0.00392 Pa•s

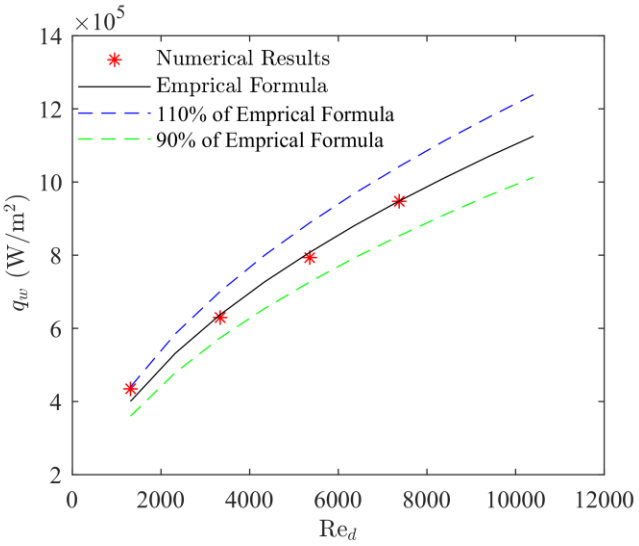

Figure 5 Comparison of numerical results and empirical formula

Based on the definition, the Prandtl number of the ATF is calculated as

$$\mathrm{Pr} = \frac{C_p\mu}{k} = 67.45 \tag{2}$$

The jet Reynolds number is calculated based on the jet exit diameter as

$$\mathrm{Re}_d = \frac{\rho v d}{\mu} \tag{3}$$

Utilizing the definition of the Nusselt number, the stagnation zone wall heat flux from the empirical formula is calculated using the following equation

$$q_w = \frac{k\left(T_w - T_f\right)\mathrm{Nu}_d}{d} \tag{4}$$

Four different numerical cases with the Reynolds number of $\mathrm{Re}_d = 1314, 3334, 5354, 7375$ are simulated to validate the numerical results. The Reynolds number is varied by changing inlet velocities. The maximum wall heat flux from the numerical simulations and the computations from the empirical formula are compared. The results are shown in Fig. 5. It could be seen that a good agreement of the numerical results and the empirical formula is achieved. The numerical results fall in the $\pm 10\%$ bounds of the empirical formula. Therefore, it could be concluded that the numerical code used in the current study is correctly implemented.

Comparison with Experimental Measurements

The developed numerical model for heat transfer performance prediction is compared against experimental measurement data [14]. In [14], Choi et.al. carried out the experimental measurement of a slot-jet impingement on a semi-circular surface with air as working fluid. The mesh which is shown in Fig. 3 is used to perform the comparative CFD simulation. The working fluid is changed to air following the experimental setup in [14]. In the present study, the inlet velocity is changed by matching the jet exit Reynolds number used in [14], which is $\mathrm{Re} = 4740$. A constant temperature of $T_f = 300\mathrm{K}$ at the inlet boundary is specified. The no-slip constant heat flux (5000 W/m^2) wall boundary condition is adopted. The pressure outlet boundary condition is utilized with the gauge pressure as zero. Though the setup in [14] and the present study are similar, the geometric parameters are different. The normalized local Nusselt number is defined as

$$\widehat{\mathrm{Nu}}_d = \frac{\mathrm{Nu}_d - \mathrm{Nu}_d^{\min}}{\mathrm{Nu}_d^{\max} - \mathrm{Nu}_d^{\min}} \tag{5}$$

to have a fair comparison of the results, where $\mathrm{Nu}_d^{\max}$ and $\mathrm{Nu}_d^{\min}$ are the maximum and minimum values of the local Nusselt number, respectively. The comparative results of the CFD simulation in the present study and experimental measurements in [14] is shown in Fig. 6, where r is the radius of the jet exit. It could be seen from Fig. 6 that reasonable agreement between the CFD simulation and the experimental measurements is achieved.

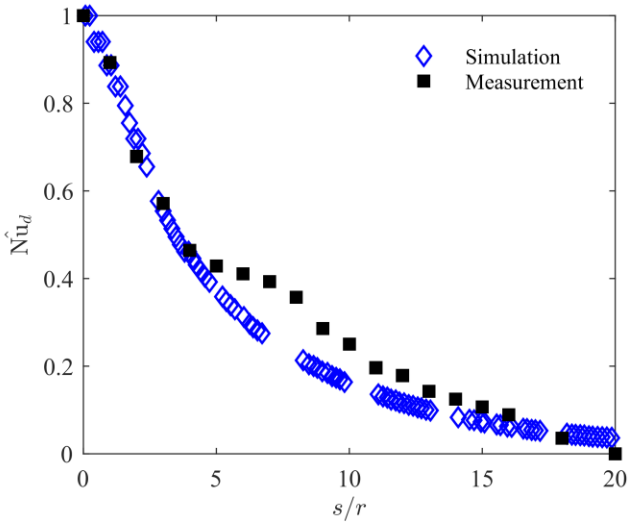

Figure 6 Comparison with measurements in [14]

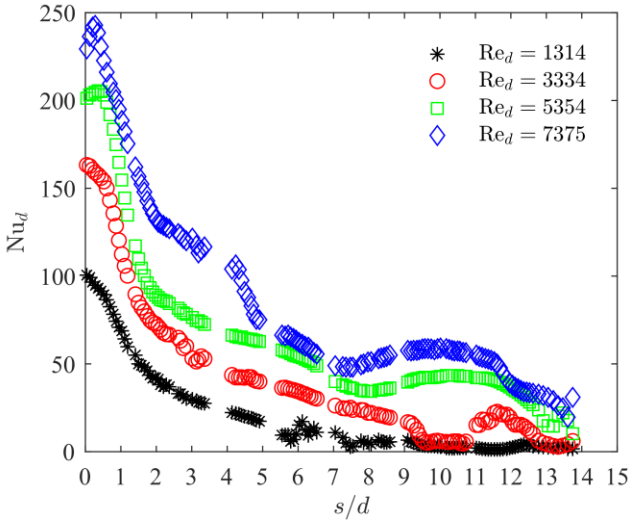

Figure 8 Local Nusselt number distribution for different Reynolds number

Parametric Study and Discussion

The parametric investigation regarding the cooling performance of the developed jet impingement system is conducted by selecting a set of relevant parameters. These parameters are four different Reynolds numbers, $\mathrm{Re}_d = 1314, 3334, 5354, 7375$ and five pipe rotation speeds, $\Omega = 0\ \mathrm{rpm}, 1000\ \mathrm{rpm}, 2000\ \mathrm{rpm}, 3000\ \mathrm{rpm}, 4000\ \mathrm{rpm}$. These parameters result in a combination of 20 different numerical cases regarding the jet impingement cooling system. In order to validate the effect of jet exit Reynolds number on the heat transfer performance, the numerical cases with zero rotation speed and four different Reynolds numbers are carried out. The distribution of the wall heat flux results is shown in Fig. 7. The results of the local Nusselt numbers along the dimensionless length s/d are plotted in Fig. 8. Figures 7 and 8 show the significant effect of jet exit Reynolds number on the cooling performance of the jet impingement system. It could be seen from Fig. 8 that the Nusselt number is highest at the stagnation zone. The variations of the Nusselt numbers in the stagnation zone are small, which is consistent with the statement in [7] that the changes of Nusselt number are within 10% in the zone of $\frac{s}{d} < 0.7$. The local Nusselt number at larger dimensionless length decreases very rapidly. For high Reynolds numbers, i.e. $\mathrm{Re}_d = 5354, 7375$, the peaks of the Nusselt number occur slightly away from the stagnation point, where $\frac{s}{d} = 0$. The enhancement of heat transfer performance due to the increase of the Reynolds number can be attributed to the increase of mass flow rate and associated convective heat transfer strength.

The effect of rotation on the heat transfer performance is investigated by conducting the numerical cases of different rotation speeds. The volume fractions of the ATF for different Reynolds numbers and rotation speeds are shown in Fig. 9. Two phenomena could be observed from Fig. 9. First, the impingement flow field is distorted due to the rotation. Second,

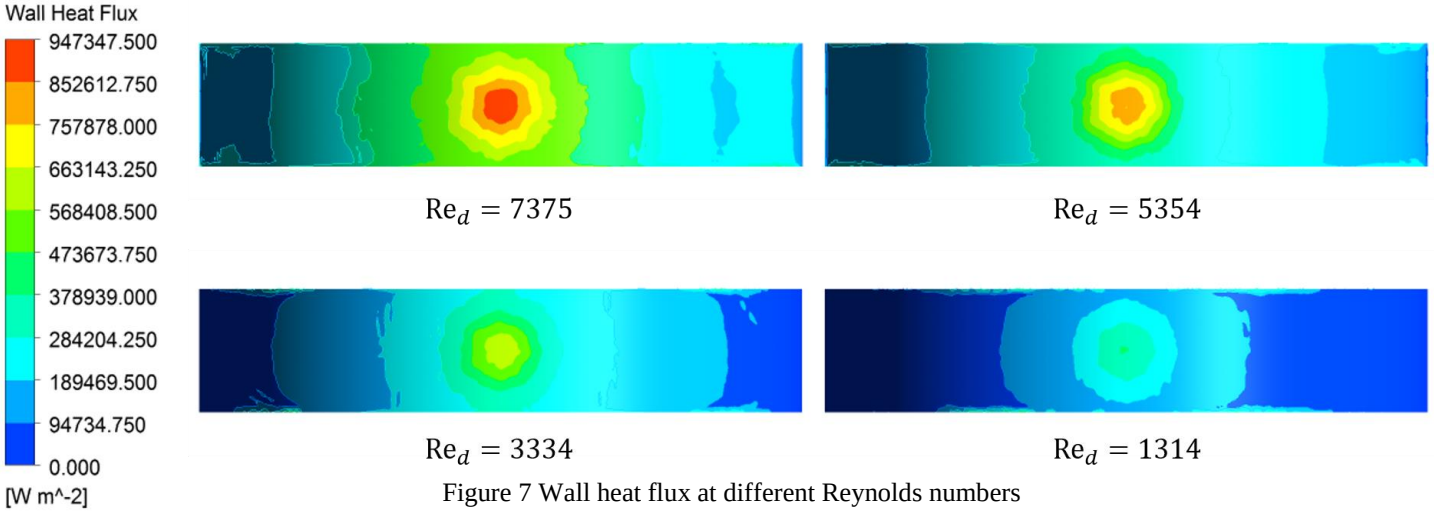

Figure 7 Wall heat flux at different Reynolds numbers

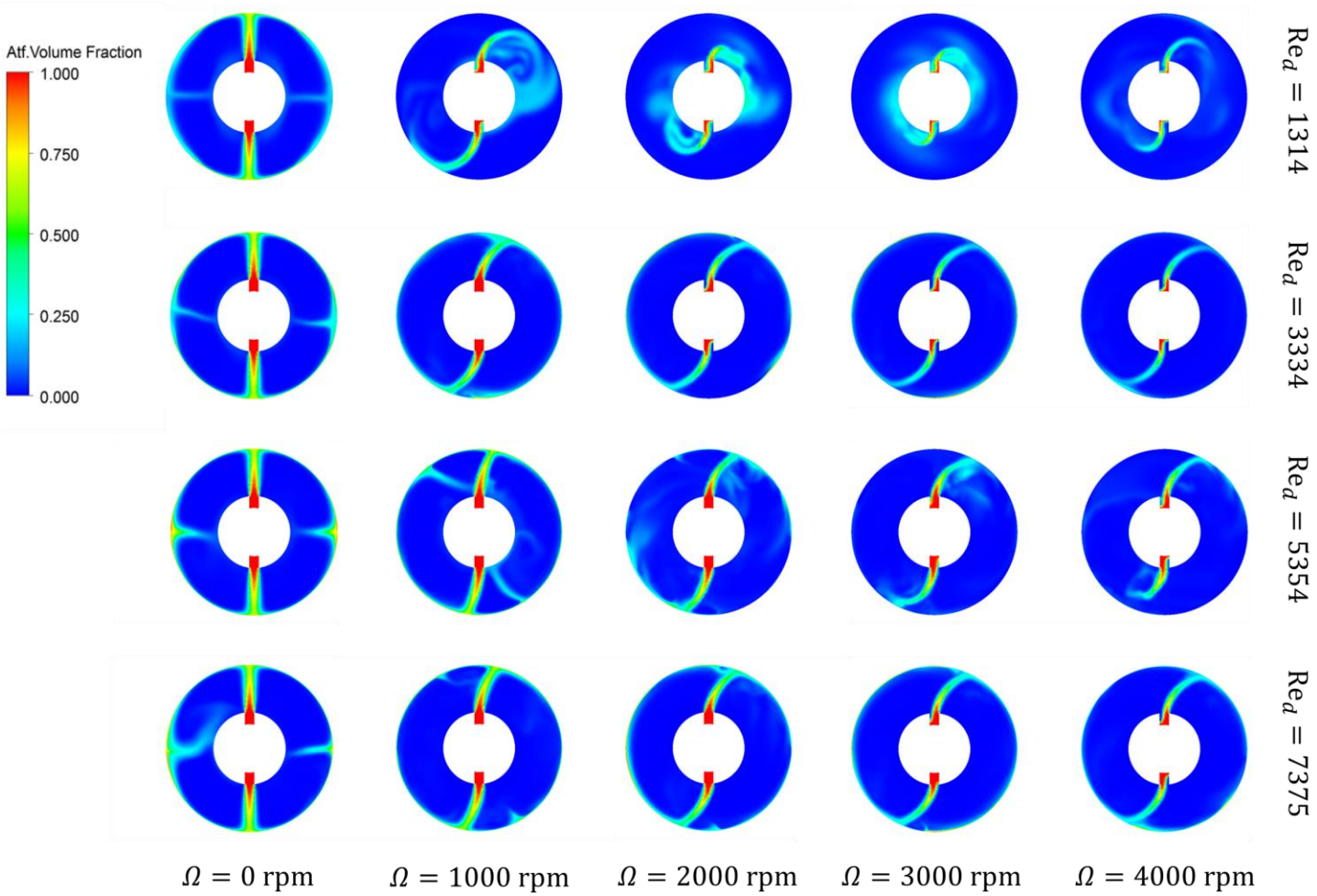

Figure 9 Volume fraction of ATF for different Reynolds numbers and rotation speeds

in the case of high speed rotation and low Reynolds number, the impinging ATF may not be able to hit the hot surface.

The overall cooling performance of the jet impingement system can be quantified by the average Nusselt number, $\overline{\mathrm{Nu}_d}$, which is calculated by taking the area weighted average of the local Nusselt number over the cylindrical wall. The variations of the average Nusselt number due to the different rotation speeds are shown in Fig. 10. With the increase of the rotation speed, the average Nusselt number decreases monotonically for all Reynolds numbers. Furthermore, the increase of the Reynolds number leads to the increase of the average Nusselt number. However, some special cases may occur in the high-speed rotation region. For example, the average Nusselt number for $\mathrm{Re}_d = 5354, \Omega = 3000\mathrm{rpm}$ case is lower than the case of $\mathrm{Re}_d = 3334, \Omega = 3000\mathrm{rpm}$. This may be due to the fact that the high-speed rotation leads to the separation of the impinging flow and the target surface, which is consistent with the observation from the results shown in Fig. 9.

Though the average Nusselt number is decreasing, this phenomenon does not conflict with the motivation of the pipe rotation. The motivation for the rotational pipe is to ensure the

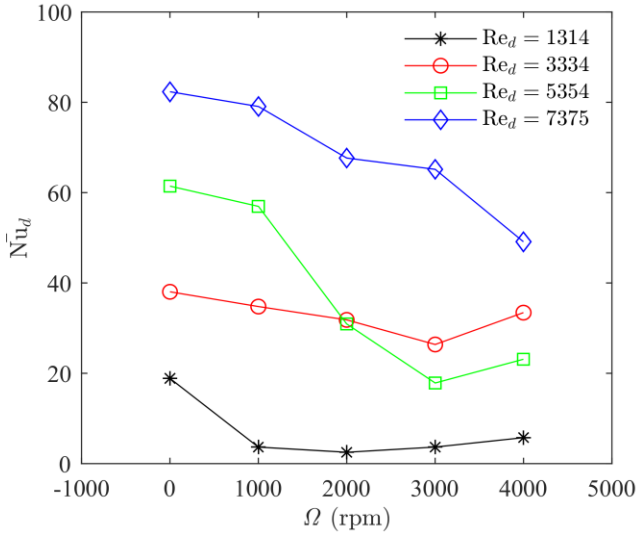

Figure 10 Average Nusselt number

uniform heat removal on the cylindrical ring. If the pipe remains static, the heat removal performance remains satisfactory near two stagnation zone regions while in other regions, the undesirable heat accumulation may occur. Thus, the uniformity of the overall heat removal performance is quantified by the area weighted standard deviation of the Nusselt number, σ_{Nu_d}. The results of σ_{Nu_d} due to different rotation speeds and Reynolds number are shown in Fig. 11. It could be seen from Fig. 11

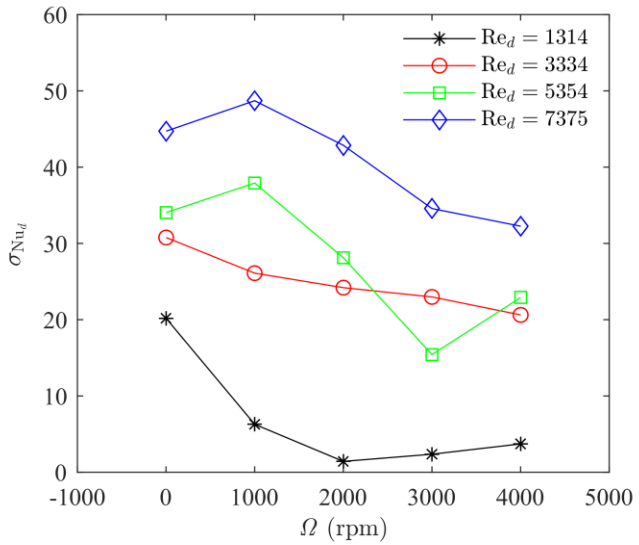

Figure 11 Standard deviation of the Nusselt number

that the overall trend of the standard deviation is decreasing with the increasing of the rotation speeds, which means that the uniformity of the heat removal performance could be achieved with the increasing of the rotation speeds. However, there are two points should be noted. First, for low rotation speeds and high Reynolds number configuration, the standard deviation may increase. This increase may be due to slight distortion of the impingement flow, which leads to the shift of the stagnation zone to one half, resulting in the concentration of the flow field. Second, the standard deviation may increase in the high-speed region. This is because the separation of the impingement flow from the target. Therefore, it could be concluded that for a specific jet Reynolds number, there should be a range of suitable speeds. In the suitable rotational speed range, the uniformity of the heat removal performance could be achieved with the increasing of the rotational speed.

The correlation of the average Nusselt number and other relevant parameters is developed, where some outliers are eliminated from the correlation. The functional relationship is described using the following equation

$$\overline{\mathrm{Nu}_d} = 0.02527\,\mathrm{Re}_d^{0.9071} - 0.0003576\Omega^{1.358} \qquad (6)$$

The developed correlation and the simulation results are compared in Fig. 12. It could be seen that except some extreme low Nusselt number points, the overall fitness of the developed correlation is acceptable. Increasing the Reynolds number

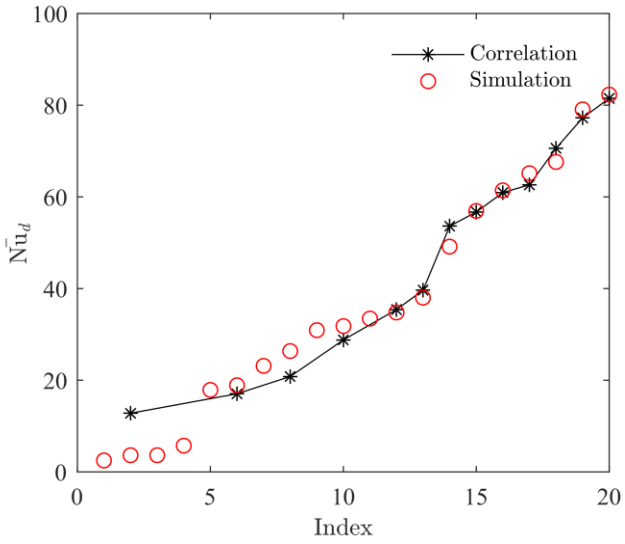

Figure 12 Comparison of correlation and simulation results

enhances the heat removal performance, while the Nusselt number varies reversely with the increase of the rotation speeds. To achieve the desired uniform cooling performance requirement, it would be necessary to consider both parameters at the same time. The correlation relationship developed in this paper could be used as guidelines to select Reynolds number and rotation speed for attaining the desired overall heat removal performance.

CONCLUSIONS

In this paper, the cooling performance of a novel rotary jet impingement system was numerically investigated. The grid sensitivity analysis was performed to obtain the grid-independent numerical results. The correctness of the numerical results was successfully validated through comparison with the empirical formula. Acceptable agreement of the numerical results and the experimental measurements was also achieved. Parametric studies of jet exit Reynolds number and rotation speeds were carried out, which include 20 different cases. The simulation results were presented with the local Nusselt number distribution, the volume fraction of ATF, the average Nusselt number and the standard deviation of the Nusselt number. The main conclusions of this paper could be summarized as follows:

1. The increase of the Reynolds number has direct impact on the heat transfer performance of the jet impingement cooling system. Higher local and average Nusselt number could be achieved with the increase of the Reynolds number.
2. The pipe rotation leads to the distortion of the impinging flow field. For high speed configurations, the separation between the impinging flow and target surface may happen.
3. Within the suitable rotational speed range, the average Nusselt number is decreasing with the increase of the pipe rotational speed. The uniformity of the heat

removal performance is enhanced with the increasing of the pipe rotational speed.

4. The correlation of the average Nusselt numbers, Reynolds numbers and pipe rotation speeds are developed, which may work as guidelines for selecting Reynolds numbers and rotation speeds when the desired overall heat removal performance is specified.

ACKNOWLEDGMENTS

The authors would like to thank all the reviewers for their insightful and constructive comments, which have helped improve the quality of the paper.

REFERENCES

[1] Gould, Kyle, Cai, Q., Steve, Neft, Charles and Bhunia, Avijit. "Liquid Jet Impingement Cooling of a Silicon Carbide Power Conversion Module for Vehicle Applications" *IEEE Transactions on Power Electronics* Vol. 30, No. 6 (2015): pp. 2975-2984.

[2] Gillot, Charlotte, Schaeffer, Christian, and Bricard, Alain. "Integrated Micro Heat Sink for Power Multichip Module" *IEEE Transactions on Industry Applications* Vol. 36, No. 1 (2000): pp. 217-221.

[3] Mertens, Robert G., Chow, Louis, Sundaram, Kalpathy B., Cregger, R. Brian, Rini, Daniel P., Turek, Louis, and Saarloos, Benjamin A. "Spray Cooling of IGBT Devices" *Journal of Electronic Packaging* Vol. 129, No. 3 (2007): pp. 316-323.

[4] Rybicki, Jon R., and Mudawar, Issam. "Single-phase and Two-phase Cooling Characteristics of Upward-facing And Downward-facing Sprays" *International Journal of Heat and Mass Transfer* Vol. 49, No. 1-2 (2006): pp. 5-16.

[5] Bhunia, Sourav K. "Impingement Splattering and Surface Disturbance Evolution on Turbulent Liquid Jets in Gases" Ph.D. Thesis, Massachusetts Institute of Technology, Cambridge, MA, 1993.

[6] Rau, Matthew J. "Turbulent Liquid-vapor Flow Interactions and Heat Transfer in Confined Jet Impingement Boiling" Ph.D. Thesis, Purdue University, West Lafayette, IN, 2016.

[7] Lienhard, John H. "Heat Transfer by Impingement of Circular Free-Surface Liquid Jets" in *Proceedings of 18th National and 7th ISHMT-ASME Heat and Mass Transfer Conference,* Guwahati, India, January 4-6, 2006.

[8] Zhao, Zenghui, Woodcock, Corey, Peles, Yoav, and Jensen, Michael K. "Enhanced Liquid Jet Impingement Boiling" in *Proceedings of ASME International Mechanical Engineering Congress and Exposition*, IMECE2012-89265: pp. 2869-2875. Houston, TX, November 9–15, 2012.

[9] Maysam, Molana, and Banooni, Salem. "Investigation of Heat Transfer Processes Involved Liquid Impingement Jets: A Review" *Brazilian Journal of Chemical Engineering,* Vol. 30, No. 3 (2013): pp. 413-435.

[10] Stevens, J. and Webb, Brent W. "Local Heat Transfer Coefficients Under an Axisymmetric, Single-Phase Liquid Jet" *ASME Journal of Heat Transfer* Vol. 113, No. 1 (1991): pp. 71-78.

[11] Sharif, M. A. R. and Mothe, K. K. "Parametric Study of Turbulent Slot-jet Impingement Heat Transfer from Concave Cylindrical Surfaces" *International Journal of Thermal Sciences* Vol. 49, No. 2 (2010): pp. 428-442.

[12] Taghinia, Javad, Rahman, Md Mizanur, and Siikonen, Timo. "CFD Study of Turbulent Jet Impingement on Curved Surface" *Chinese Journal of Chemical Engineering,* Vol. 24, No. 5 (2016): pp. 588-596.

[13] Choi, Mansoo, Yoo, Han Seoung, Yang, Geunyoung, Lee, Joon Sik, and Sohn, Dong Kee. "Measurements Of Impinging Jet Flow and Heat Transfer on a Semi-Circular Concave Surface" *International Journal of Heat and Mass Transfer* Vol. 43, No. 10 (2000): pp. 1811-1822.

[14] Rahman, Muhammad M., Lallave, Jorge C., and Kumar, Ashok. "Heat Transfer from a Spinning Disk During Semi-Confined Axial Impingement From a Rotating Nozzle" *International Journal of Heat and Mass Transfer,* Vol. 51, No. 17-18 (2008): pp. 4400-4414.

[15] Sagot, Benoit, Antonini, G., Christgen, A., and Buron, Franck. "Jet Impingement Heat Transfer on a Flat Plate at a Constant Wall Temperature" *International Journal of Thermal Sciences,* Vol. 47, No. 12 (2008): pp. 1610-1619.

[16] Bostjan, Koncar, Draksler, M., Oblak, K., Norajitra, P., and Widak, V., "Numerical Investigation of Multiple-Jet Cooling Concept for Helium Cooled Divertor" in *Proceedings of International Conference Nuclear Energy for New Europe*, Portoroz, Slovenia, Sept. 8-11, 2008.

[17] Kemp, Steven P., and Linden, James L. "Physical and Chemical Properties of a Typical Automatic Transmission Fluid" in *Proceedings of International Fuels and Lubricants Meeting and Exposition,* No. 902148, Tulsa, OK, October 22-25, 1990.